Chapter 11
Partial Differential Equations

11.1 Introduction

This section discusses some fundamental aspects of the numerics of partial differential equations and it will be restricted to methods already encountered in previous chapters, i.e. on finite difference methods. These are particularly useful to find solutions of linear partial differential equations (PDEs). Nonlinear PDEs, such as the NAVIER-STOKES equations, require more advanced techniques as there are finite element methods or finite volume methods for conservation laws. A detailed discussion of a wide spectrum of methods can be found in many textbooks on the numerics of PDEs the interested reader is referred to [1–7].

Since we already introduced the concepts of finite difference derivatives in Chap. 2 and their application to boundary value problems of ordinary differential equations in Sect. 8.2, we concentrate mainly on the application of these methods to specific types of PDEs. In detail, we investigate the POISSON equation as an example for *elliptic PDEs*, the time dependent heat equation as an example for *parabolic PDEs*, and the wave equation as an example for *hyperbolic PDEs*. The concepts presented here are, of course, also applicable to other problems. However, in contrast to the numerics of ordinary differential equations, there exists no general recipe for the solution of PDEs.

Another important point to note is that, as in the theory of ordinary differential equations, the problem is only fully determined when initial and/or boundary conditions have been defined. For instance, in the case of the POISSON equation only boundary conditions are required, while for the time-dependent heat equation initial conditions are required as well. In general, pure boundary value problems are easier from a numerical point of view because the question whether or not the algorithm is stable does not play such an important role. For combined boundary

B.A. Stickler, E. Schachinger, *Basic Concepts in Computational Physics*,
DOI 10.1007/978-3-319-27265-8_11

and initial value problems it is essential to check carefully that the discretization of the time axis is not in conflict with the discretization of the space domain. This is of particular importance in the numerical treatment of hyperbolic PDEs, where the so called COURANT-FRIEDRICHS-LEWY (CFL) condition determines the stability of the algorithm. We shall come back to this point in Sects. 11.3 and 11.4. Finally, we conclude this chapter with a discussion of the numerical solution of the time-dependent SCHRÖDINGER equation.

11.2 The POISSON Equation

We consider the POISSON equation as a model for an elliptic PDE [8, 9]. Nevertheless, we review briefly some basics of electrodynamics [10, 11]. The force $F(r,t)$ as a function of position $r \in \mathbb{R}^3$ and time $t \in \mathbb{R}^+$ acting on a particle with charge q, which moves with velocity v within an electromagnetic field described by the electric field $E(r,t)$ and the magnetic field $B(r,t)$, is determined from:

$$F(r,t) = q\left[E(r,t) + v \times B(r,t)\right] \; . \tag{11.1}$$

We consider here the electrostatic case which is characterized by a zero magnetic field $[B(r,t) = 0]$ and a time independent electric field. The electric field E itself is described by the equation

$$\nabla \cdot E(r) = \frac{1}{\epsilon_0}\rho(r) \; , \tag{11.2}$$

where the charge density $\rho(r,t)$ acts as the source of the electric field $E(r,t)$. Here ϵ_0 is the dielectric permittivity of vacuum. Furthermore, the electric field E is connected to the electrostatic potential $\varphi(r)$ via

$$E(r) = -\nabla\varphi(r) \; . \tag{11.3}$$

Thus, Eq. (11.2) is reformulated as:

$$\Delta\varphi(r) = -\frac{\rho(r)}{\epsilon_0} \; . \tag{11.4}$$

This equation is referred to as the POISSON equation and in the particular case of $\rho(r) = 0$ it is referred to as the LAPLACE equation [12].

We focus now on the numerical solution of the two dimensional POISSON equation (11.4) on a rectangular domain $\Omega = [0, L_x] \times [0, L_y]$ together with boundary conditions $\varphi(x, y) = g(x, y)$ on $\partial\Omega$. In detail, we want to solve the two-dimensional boundary value problem

$$\begin{cases} \frac{\partial^2}{\partial x^2}\varphi(x,y) + \frac{\partial^2}{\partial y^2}\varphi(x,y) = -\rho(x,y) \ , & (x,y) \in \Omega \ , \\ \varphi(x,y) = g(x,y) \ , & (x,y) \in \partial\Omega \ , \end{cases} \tag{11.5}$$

where we absorbed ϵ_0 into the charge density $\rho(x, y)$. Note that a treatment of the three dimensional case can be carried out in analogue.

We employ a finite difference approximation to the derivatives which appear in Eq. (11.5) (see Chap. 2) and we define grid-points in x and y direction via

$$x_i = x_0 + ih_x, \quad i = 0, 1, 2, \ldots, n \ , \tag{11.6a}$$

$$y_j = y_0 + jh_y, \quad j = 0, 1, 2, \ldots, m \ , \tag{11.6b}$$

where h_x and h_y denote the grid-spacing in x- and y-direction, respectively. As discussed in Chap. 2 we consider only equally spaced grid-points. An extension to non-uniform grids is straight forward.

We define the function values on the grid-points as

$$\varphi_{i,j} \equiv \varphi(x_i, y_j) \ , \tag{11.7}$$

and similarly $\rho_{i,j} \equiv \rho(x_i, y_j)$. Consequently, we find the finite difference approximation of Eq. (11.5):

$$\frac{\varphi_{i-1,j} - 2\varphi_{i,j} + \varphi_{i+1,j}}{h_x^2} + \frac{\varphi_{i,j-1} - 2\varphi_{i,j} + \varphi_{i,j+1}}{h_y^2} = -\rho_{i,j} \ . \tag{11.8}$$

The boundary conditions (11.5) can be written as

$$\varphi_{0,j} = g_{0,j} \ , \quad j = 0, 1, \ldots, m \ , \tag{11.9a}$$

$$\varphi_{n,j} = g_{n,j} \ , \quad j = 0, 1, \ldots, m \ , \tag{11.9b}$$

$$\varphi_{i,0} = g_{i,0} \ , \quad i = 1, 2, \ldots, n-1 \ , \tag{11.9c}$$

$$\varphi_{i,m} = g_{i,m} \ , \quad i = 1, 2, \ldots, n-1 \ . \tag{11.9d}$$

Equation (11.8) is multiplied by $-h_x^2 h_y^2/2$ and we obtain after rearranging terms

$$\left(h_x^2 + h_y^2\right) \varphi_{i,j} - \frac{1}{2}\left[h_y^2\left(\varphi_{i-1,j} + \varphi_{i+1,j}\right) + h_x^2\left(\varphi_{i,j-1} + \varphi_{i,j+1}\right)\right] = \frac{(h_x h_y)^2}{2}\rho_{i,j} , \tag{11.10}$$

for $i = 1, \ldots, n$ and $j = 1, \ldots, m$. There are different strategies how this set of equations might be solved. The common strategy is to employ the assignments

$$\begin{aligned} \varphi_{1,1} &\to \varphi_1 , \\ \varphi_{1,2} &\to \varphi_2 , \\ \vdots \quad & \quad \vdots \\ \varphi_{n,m} &\to \varphi_\ell , \end{aligned} \tag{11.11}$$

where $\ell = nm$. Equation (11.10) is then rewritten as a matrix equation with a vector of unknowns $\varphi = (\varphi_1, \varphi_2, \ldots, \varphi_\ell)^T$ according to Eq. (11.11). The boundary conditions are to be included in the matrix. This matrix equation is then solved either by direct or iterative methods as they are discussed in Appendix C.

It is our plan to solve Eq. (11.10) iteratively. This requires the introduction of a superscript iteration index t and $\varphi_{i,j}^t$ denotes the function value $\varphi(x_i, y_j)$ after t-iteration steps. There are two different implementations of an iterative solution, namely the GAUSS-SEIDEL or the JACOBI method (Appendix C). They differ only in the update procedure of the function values $\varphi_{i,j}^t$ at the grid-points. The basic idea is to develop an update algorithm which expresses the function values $\varphi_{i,j}^t$ with the help of function values at already updated grid-points and of function values $\varphi_{i,j}^{t-1}$ determined in the preceding iteration step [Appendix, Eq. (C.27)].

We formulate this iteration rule as

$$\begin{aligned} \varphi_{i,j}^{t+1} = {} & \frac{(h_x h_y)^2}{2(h_x^2 + h_y^2)}\rho_{i,j} + \frac{1}{2(h_x^2 + h_y^2)}\left[h_y^2\left(\varphi_{i-1,j}^{t+1} + \varphi_{i+1,j}^t\right)\right. \\ & \left. + h_x^2\left(\varphi_{i,j-1}^{t+1} + \varphi_{i,j+1}^t\right)\right] , \end{aligned} \tag{11.12}$$

where we abstained from incorporating a relaxation parameter (see Appendix C). Note that by using the iteration rule (11.12) the boundary conditions have to be accounted for in an additional step.

Let us specify the boundary conditions for a concrete problem: We we want to determine the electrostatic potential of an electric monopole, dipole, and quadrupole, respectively. They are placed inside a grounded box of dimensions L_x and L_y. Thus, we have to impose DIRICHLET boundary conditions $\varphi(0, y) = \varphi(L_x, y) = 0$ in x-direction and $\varphi(x, 0) = \varphi(x, L_y) = 0$ in y-direction. In this particular case the boundary conditions can be made part of Eq. (11.12) by restricting the loop over the x-grid (y-grid) to $i = 2, \ldots, N - 1$ which leaves the boundary points $\varphi(0, y)$ [$\varphi(x, 0)$] and $\varphi(L_x, y)$ [$\varphi(x, L_y)$] unchanged. Furthermore we set $L_x = L_y = 10$, the number of grid-points on both axes to $n = m = 100$, and define the domains:

$$\Omega_1 = \left(x_{\frac{n}{2}-10}, x_{\frac{n}{2}}\right] \times \left(y_{\frac{m}{2}-10}, y_{\frac{m}{2}}\right] \ , \tag{11.13a}$$

$$\Omega_2 = \left(x_{\frac{n}{2}}, x_{\frac{n}{2}+10}\right] \times \left(y_{\frac{m}{2}-10}, y_{\frac{m}{2}}\right] \ , \tag{11.13b}$$

$$\Omega_3 = \left(x_{\frac{n}{2}-10}, x_{\frac{n}{2}}\right] \times \left(y_{\frac{m}{2}}, y_{\frac{m}{2}+10}\right] \ , \tag{11.13c}$$

$$\Omega_4 = \left(x_{\frac{n}{2}}, x_{\frac{n}{2}+10}\right] \times \left(y_{\frac{m}{2}}, y_{\frac{m}{2}+10}\right] \ . \tag{11.13d}$$

The charge density $\rho(x, y)$ is described by three different scenarios, namely the electric monopole

$$\rho_1(x, y) = \begin{cases} 50 & (x, y) \in \Omega_1 \cup \Omega_2 \cup \Omega_3 \cup \Omega_4 \ , \\ 0 & \text{elsewhere,} \end{cases} \tag{11.14a}$$

the electric dipole

$$\rho_2(x, y) = \begin{cases} 50 & (x, y) \in \Omega_1 \cup \Omega_2 \ , \\ -50 & (x, y) \in \Omega_3 \cup \Omega_4 \ , \\ 0 & \text{elsewhere,} \end{cases} \tag{11.14b}$$

and the electric quadrupole:

$$\rho_3(x, y) = \begin{cases} 50 & (x, y) \in \Omega_1 \cup \Omega_4 \ , \\ -50 & (x, y) \in \Omega_2 \cup \Omega_3 \ , \\ 0 & \text{elsewhere.} \end{cases} \tag{11.14c}$$

These charge densities are illustrated in Fig. 11.1.

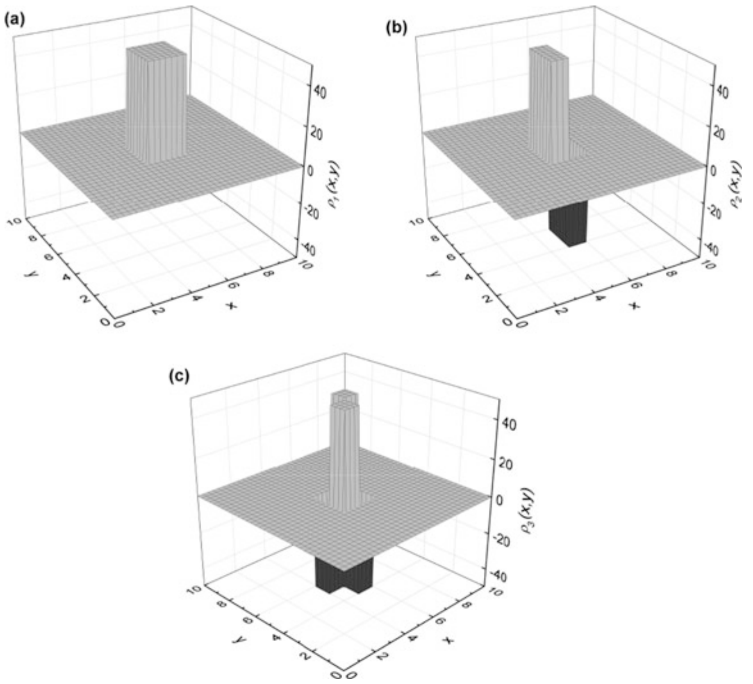

Fig. 11.1 The electric monopole, dipole, and quadrupole charge densities **(a)** $\rho_1(x,y)$, **(b)** $\rho_2(x,y)$, and **(c)** $\rho_3(x,y)$, respectively, as defined in Eq. (11.14)

The solution of Eq. (11.12) is regarded to be converged if the potential $\varphi(x,y)$ does not change significantly between two consecutive iteration steps, i.e.

$$\max_{i,j}\left(|\varphi_{i,j}^{t}-\varphi_{i,j}^{t-1}|\right)<\eta\ , \tag{11.15}$$

where $\eta = 10^{-4}$ is the required accuracy. A criterion to check the relative change can be formulated in a similar fashion. The resulting potential profiles $\varphi(x,y)$ are presented in Fig. 11.2. They reflect perfectly the symmetries of the charge densities $\rho_1(x,y)$, $\rho_2(x,y)$, and $\rho_3(x,y)$, respectively. Finally, standard finite difference methods can be applied to calculate, based on Eq. (11.3), the electric field $E(x,y)$ from the potential profiles $\varphi(x,y)$.[1]

[1] We note that the electrostatic potentials that we calculated here numerically can also be determined analytically with the method of mirror charges [10].

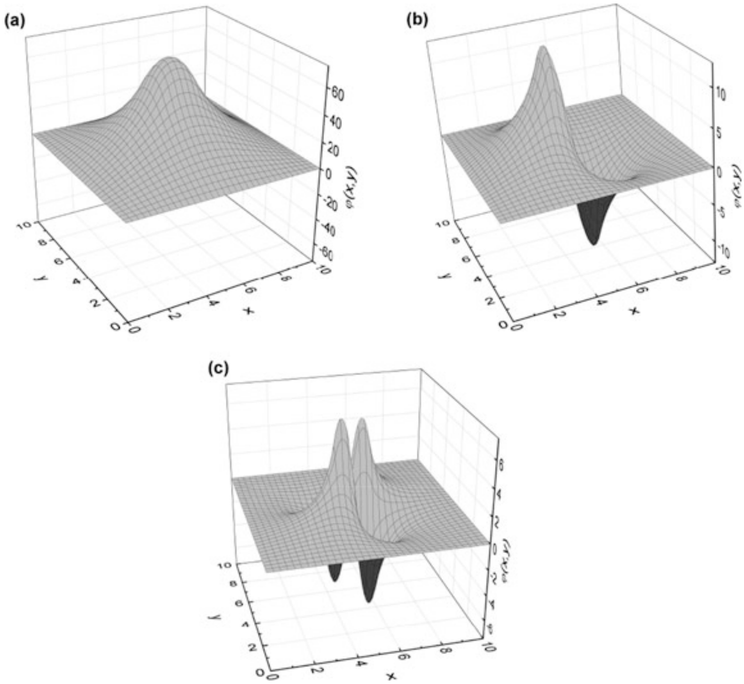

Fig. 11.2 Potential profile $\varphi(x, y)$ obtained for charge density **(a)** $\rho_1(x, y)$, **(b)** $\rho_2(x, y)$, and **(c)** $\rho_3(x, y)$

11.3 The Time-Dependent Heat Equation

We discuss here the numerical solution of the time-dependent heat equation [13, 14] which is a representative of parabolic PDEs. This equation has already been introduced in Sect. 9.1, Eq. (9.1), and is, reduced to the one-dimensional case, of the form

$$\frac{\partial}{\partial t} T(x, t) = \kappa \frac{\partial^2}{\partial x^2} T(x, t) \ , \tag{11.16}$$

with the thermal diffusivity κ. It is augmented by appropriate boundary and initial conditions. Again, we will not discuss the extension to higher dimensions since it is straight forward, however, maybe tedious in the general case. We approximate the right hand side of Eq. (11.16) with the help of the central finite difference approximation (Sect. 2.2) and obtain

$$\frac{\partial}{\partial t} T_k(t) = \kappa \frac{T_{k-1}(t) - 2T_k(t) + T_{k+1}(t)}{h^2} \ , \tag{11.17}$$

with the usual discretization $x_k = x_0 + kh$, $k = 0, \dots, N$, in combination with the notation $T_k(t) \equiv T(x_k, t)$.

The time derivative in Eq. (11.17) can be approximated with the help of methods already discussed in Chap. 5. In particular, one has to decide whether the solution of Eq. (11.17) should be approximated by an explicit or an implicit integrator. In order to emphasize the differences between the two methods, the application of the explicit EULER and of the implicit EULER method will be studied. However, more complex integrators may be applied as well. In particular, the CRANK-NICOLSON method [15] proved to be very useful for the solution of parabolic differential equations.

We define $t_n = t_0 + n\Delta t$ and $T_k^n \equiv T_k(t_n)$ and employ the explicit EULER scheme (5.9) in Eq. (11.17) to get

$$\frac{T_k^{n+1} - T_k^n}{\Delta t} = \kappa \frac{T_{k-1}^n - 2T_k^n + T_{k+1}^n}{h^2} , \tag{11.18}$$

with the solution:

$$T_k^{n+1} = T_k^n + \kappa \Delta t \frac{T_{k-1}^n - 2T_k^n + T_{k+1}^n}{h^2} . \tag{11.19}$$

The right hand side of this equation depends only on temperatures of the previous time step, since we used an explicit method. Although this might seem advantageous on a first glance, it turns out that the above scheme is not stable for arbitrary choices of Δt and h. In particular, it is possible to prove that the above discretization is stable only for

$$\frac{\kappa \Delta t}{h^2} \leq \frac{1}{2} . \tag{11.20}$$

A detailed discussion and proof of this property can be found in any advanced textbook on numerics of PDEs [1–5].

On the other hand, if we apply the implicit EULER method (5.10) to solve Eq. (11.17) we obtain

$$\frac{T_k^{n+1} - T_k^n}{\Delta t} = \kappa \frac{T_{k-1}^{n+1} - 2T_k^{n+1} + T_{k+1}^{n+1}}{h^2} , \tag{11.21}$$

which is unconditionally stable. However, Eq. (11.21) is an implicit equation, i.e. the function values T_{k+1}^{n+1} and T_{k-1}^{n+1} are required in order to evaluate T_k^{n+1}. Hence, Eq. (11.21) has to be solved as a system of linear equations. This system may be written as

$$AT^{n+1} = T^n + F , \tag{11.22}$$

with the vector $T^n = (T_0^n, T_1^n, \ldots, T_N^n)^T$ and the tridiagonal matrix A:

$$A = \begin{pmatrix} \ddots & \ddots & \ddots & & \\ & -\frac{\kappa \Delta t}{h^2} & 1 + \frac{2\kappa \Delta t}{h^2} & -\frac{\kappa \Delta t}{h^2} & \\ & & \ddots & \ddots & \ddots \end{pmatrix} . \tag{11.23}$$

The boundary conditions are incorporated in the matrix A and in the vector F. (See Sects. 9.2 and 9.3.) The linear system of equations (11.22) can be solved numerically using a direct or an iterative method. Employing an iterative method, imposes a third index t on the function values of the temperature T which accounts for the iteration step.

Let us give a brief numerical example. We consider the time-dependent homogeneous heat equation (11.16) on a finite interval $[0, L]$ together with the boundary conditions of Sect. 9.1:

$$T(0) = T_0, \qquad T(L) = T_N . \tag{11.24}$$

In addition we introduce the initial condition

$$T(x, 0) = 0, \qquad x \in [0, L] . \tag{11.25}$$

Figure 11.3 presents the time evolution of $T(x, t)$ at six different time-steps as it was obtained with the explicit EULER method (11.19). Here we chose $T_0 = 0$, $T_N = 2$, $N = 20$, $L = 10$, $\kappa = 1$ as well as $\Delta t \approx 0.5$. Note that for this choice of parameters, the condition (11.20) is fulfilled since $h \approx 1.05$ and therefore

$$\frac{\kappa \Delta t}{h^2} \approx 0.45 \le \frac{1}{2} . \tag{11.26}$$

Figure 11.4 corresponds to Fig. 11.3 but now Δt was chosen to be approximately 0.7 and:

$$\frac{\kappa \Delta t}{h^2} \approx 0.63 > \frac{1}{2} . \tag{11.27}$$

Thus, the stability criterion was violated and the solutions became unstable. Finally, Fig. 11.5 presents results obtained with the same parameters as for Fig. 11.4 but with the help of the implicit EULER method (11.21). Obviously, this procedure provides a stable solution of the problem.

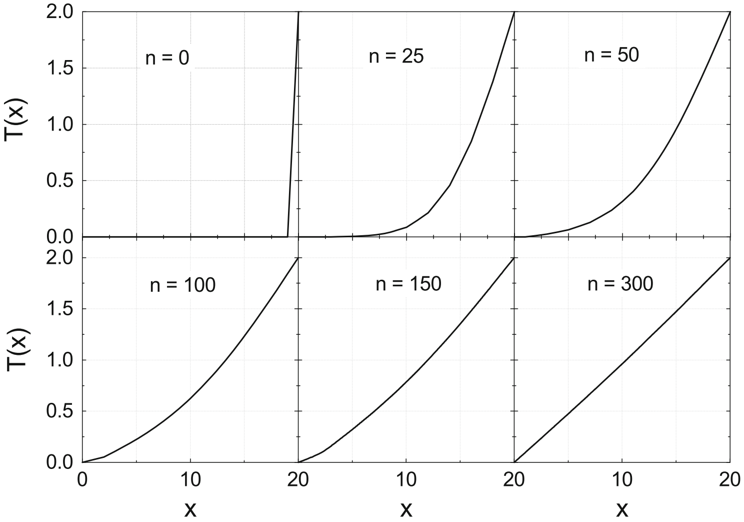

Fig. 11.3 Solutions of the time-dependent heat equation $T(x)$ vs x generated by the explicit EULER method. The stability criterion (11.20) is fulfilled. Results after $n = 25$, 50, 100, 150, and 300 time steps are presented. $n = 0$ represents the initial conditions

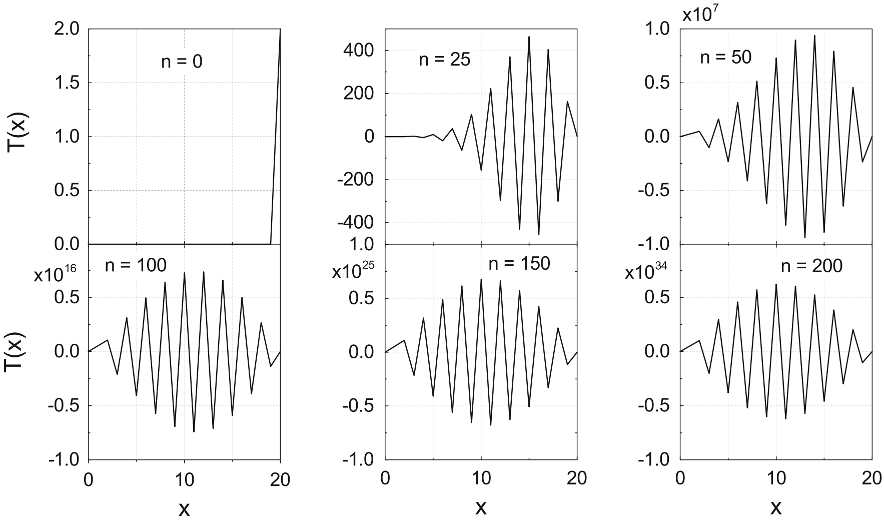

Fig. 11.4 Solutions of the time-dependent heat equation $T(x)$ vs x generated by the explicit EULER method. The stability criterion (11.20) is not fulfilled and, therefore, the solution is apparently unstable. Results after $n = 25$, 50, 100, 150, and 200 time steps are presented. $n = 0$ represents the initial conditions

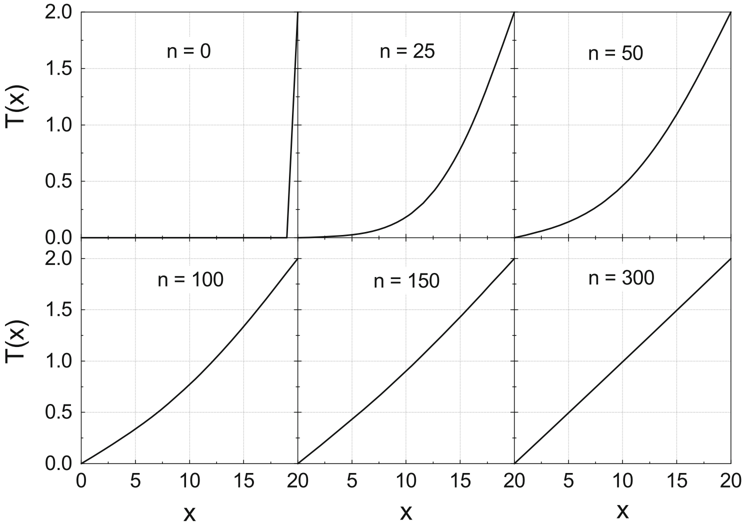

Fig. 11.5 Solutions of the time-dependent heat equation $T(x)$ vs x generated by the implicit EULER method. Results after $n = 25$, 50, 100, 150, and 300 time steps are presented. $n = 0$ represents the initial conditions

11.4 The Wave Equation

As a model hyperbolic PDE we consider briefly the wave equation [16]. Again, we regard only the one-dimensional case:

$$\frac{\partial^2}{\partial t^2} u(x,t) = c^2 \frac{\partial^2}{\partial x^2} u(x,t) \ . \tag{11.28}$$

Here, c is the speed at which the wave $u(x,t)$ propagates. Equation (11.28) is to be augmented by appropriate boundary and initial conditions. A finite difference approach similar to the one discussed in Sect. 11.3 will be employed and the discussion will be restricted to the explicit EULER approximation. Consequently, Eq. (11.28) is replaced by

$$\frac{u_k^{n-1} - 2u_k^n + u_k^{n+1}}{\Delta t^2} = c^2 \frac{u_{k-1}^n - 2u_k^n + u_{k+1}^n}{h^2} \ . \tag{11.29}$$

We define the parameter $\lambda = \frac{c\Delta t}{h}$ and solve Eq. (11.29) for u_k^{n+1}:

$$u_k^{n+1} = 2(1-\lambda^2)u_k^n - u_k^{n-1} + \lambda^2 (u_{k-1}^n + u_{k+1}^n) \ . \tag{11.30}$$

We note two important points: (i) The solution for time step $n+1$ can only be determined if the solutions for the time steps n and $n-1$ are known. In particular, the solutions for $n=0$ and $n=1$ are required to obtain the solution for $n=2$. The function values for $n=1$ can be obtained from the initial conditions which must include a first order time derivative of $u(x,t)$ since Eq. (11.28) is a second order differential equation with respect to time t. (ii) As in the case of parabolic problems, the explicit EULER approximation (11.30) will not be stable for arbitrary values of λ. It is only stable for

$$\lambda = \frac{c\Delta t}{h} \leq 1 . \tag{11.31}$$

This condition is referred to as the COURANT-FRIEDRICHS-LEWY or CFL condition [17, 18]. Its importance stems from the fact, that this condition is not limited to the wave equation but holds for hyperbolic problems in general. In particular, since the wave equation can always be viewed as a combination of a right- and a left-going advection equation, i.e.

$$\frac{\partial}{\partial t}u(x,t) = \pm c\frac{\partial}{\partial x}u(x,t) , \tag{11.32}$$

we gain the very important property that explicit time integrators applied to solve equations of the type (11.32) are only stable if relation (11.31) is obeyed.

Let us return to the discretization (11.30). Suppose we have initial conditions of the form

$$u(x,0) = f(x), \qquad \frac{\partial}{\partial t}u(x,0) = g(x) . \tag{11.33}$$

They can be approximated by

$$u_k^0 = f_k, \qquad \frac{u_k^1 - u_k^0}{\Delta t} = g_k , \tag{11.34}$$

and the solution of the second relation in (11.34) yields the desired function values for $n=1$:

$$u_k^1 = u_k^0 + \Delta t g_k . \tag{11.35}$$

However, in many cases it is beneficial to take higher order terms into account. This can be achieved by employing a TAYLOR expansion of the form (Chap. 2):

$$\frac{u_k^1 - u_k^0}{\Delta t} = \frac{\partial}{\partial t}u(x,0) + \frac{\Delta t}{2}\frac{\partial^2}{\partial t^2}u(x,0) + \mathcal{O}(\Delta t^2) . \tag{11.36}$$

We make now use of the initial conditions (11.33), employ the wave equation (11.28), and solve for u_k^1. This gives

$$u_k^1 = u_k^0 + \Delta t g_k + \frac{\Delta t^2 c^2}{2} f_k'' + \mathcal{O}(\Delta t^3) \ . \tag{11.37}$$

Here we assumed that the second spatial derivative $f_k'' = \frac{\partial^2}{\partial x^2} f(x_k)$ of the initial condition $f(x)$ exists. It may then be approximated by a finite difference approach.

To be specific we consider a vibrating string of length L, which is fixed at its ends, i.e. $u(0,t) = u(L,t) = 0$. Furthermore, we assume that the string was initially at rest, i.e.

$$\frac{\partial}{\partial t} u(x,0) = 0 \ , \tag{11.38}$$

and impose initial conditions

$$u(x,0) = \begin{cases} \sin\left(\frac{2\pi x}{L}\right) & x \in \left(\frac{L}{2}, L\right] \ , \\ 0 & \text{elsewhere.} \end{cases} \tag{11.39}$$

Figure 11.6 presents results obtained with $L = 1, c = 2, N = 100$. Δt was chosen in such a way that $\lambda = 0.5$. On the other hand, Fig. 11.7 presents calculations

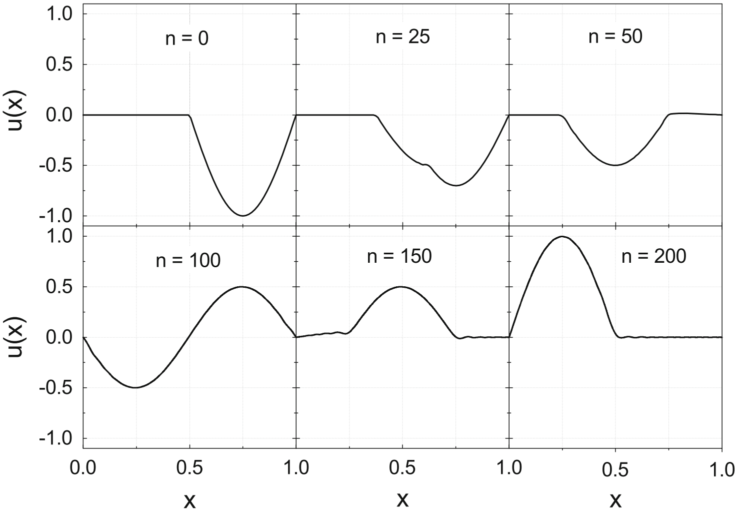

Fig. 11.6 Solutions of the wave equation $u(x)$ vs x generated by the explicit EULER method with $\lambda = 0.5$. Results after $n = 25$, 50, 100, 150, and 200 time steps are presented. $n = 0$ represents the initial conditions

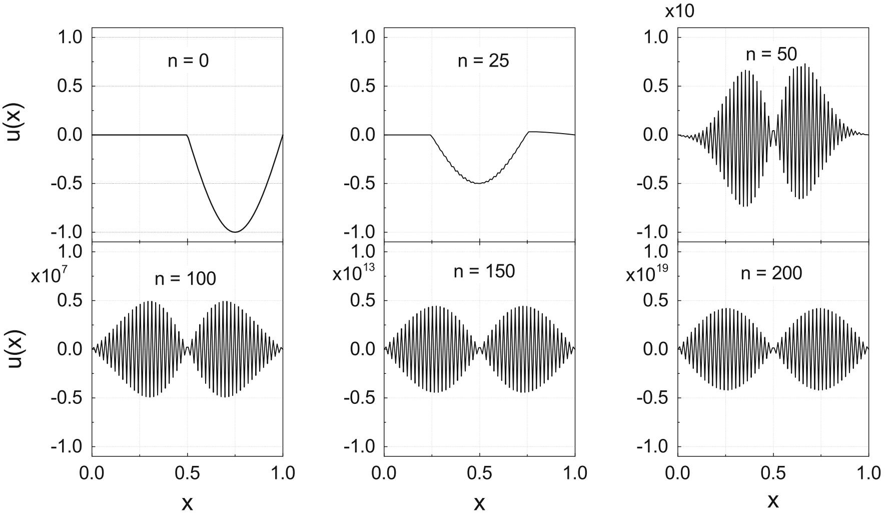

Fig. 11.7 Solutions of the wave equation $u(x)$ vs x generated by the explicit EULER method with $\lambda = 1.01$. Results after $n = 25$, 50, 100, 150, and 200 time steps are presented. $n = 0$ represents the initial conditions

performed with the same parameters but now λ was set to 1.01. Thus, the CFL condition (11.31) was violated and the solutions become unstable.

In general, the numerical solution of hyperbolic PDEs can be very difficult to obtain since in many cases these equations represent conservation laws. A very popular class of methods in this context is referred to as *finite volume methods*. A detailed discussion of these methods can be found in the book by R. J. LEVEQUE [6].

11.5 The Time-Dependent SCHRÖDINGER Equation

We already came across the time-dependent SCHRÖDINGER equation in Chap. 10. It reads

$$i\hbar \frac{\partial}{\partial t} \Psi(x, t) = H\Psi(x, t) , \tag{11.40}$$

where $\hbar$ is the reduced PLANCK constant, $\Psi(x, t)$ is the wave function, and H is the HAMILTON operator. Since the SCHRÖDINGER equation contains a complex coefficient, it cannot be categorized as a PDE of one of the familiar types, i.e. elliptic, parabolic or hyperbolic. In fact, the SCHRÖDINGER equation shows parabolic as well as hyperbolic behavior (it is of the form of the diffusion equation but allows for wave solutions). We discuss here briefly a very elegant method developed to numerically approximate solutions of the time-dependent SCHRÖDINGER equation, A prominent alternative method, the split operator technique, is briefly explained in Appendix D.

We note that Eq. (11.40) has the formal solution

$$\Psi(x,t) = \exp\left(-\frac{it}{\hbar}H\right)\Psi(x,0) = U(t)\Psi(x,0)\ , \qquad (11.41)$$

where we assumed that H is independent of time t. We note that the operator $U(t)$ on the right hand side of Eq. (11.41) *propagates* the solution in time. Furthermore, it is a unitary operator and therefore preserves the norm of the wave-function $\Psi(x,t)$. $U(t)$ is usually referred to as the *unitary time-evolution operator* [19].[2]

We employ relation (11.41) and obtain

$$\Psi(x,t+\Delta t) = \exp\left[-\frac{i(t+\Delta t)}{\hbar}H\right]\Psi(x,0) = \exp\left(-\frac{i\Delta t}{\hbar}H\right)\Psi(x,t)\ . \qquad (11.42)$$

Expanding the exponential in this equation in its series representation and truncating the series after the second term results in the approximation

$$\Psi(x,t+\Delta t) \approx \left(1-\frac{i\Delta t}{\hbar}H\right)\Psi(x,t)\ . \qquad (11.43)$$

Again, we introduce grid-spacing $x_k = k\Delta x$, $k \in \mathbb{N}$ and the correspondingly indexed functions $\Psi_k^n \equiv \Psi(x_k, n\Delta t)$ which results in

$$\Psi_k^{n+1} = \left(1-\frac{i\Delta t}{\hbar}H\right)\Psi_k^n\ . \qquad (11.44)$$

Using Eq. (10.23) for the Hamiltonian in its position space representation in the one-dimensional case and by approximating the second derivative with the help of the central difference approximation we arrive at

$$\Psi_k^{n+1} = \Psi_k^n - \frac{i\Delta t}{\hbar}\left(-\frac{\hbar^2}{2m}\frac{\Psi_{k-1}^n - 2\Psi_k^n + \Psi_{k+1}^n}{\Delta x^2} + V_k\Psi_k^n\right)\ , \qquad (11.45)$$

where we defined $V_k \equiv V(x_k)$.

The iteration scheme (11.45) resembles the explicit EULER approximation (11.18) of the heat equation with the difference that we have here an imaginary coefficient. An implicit procedure for the time-dependent SCHRÖDINGER

[2] We remember that unitary means that $UU^\dagger = U^\dagger U = \mathbb{1}$.

equation (11.40) can be obtained by inversion of Eq. (11.42):

$$\Psi(x,t) = U^{\dagger}(\Delta t)\Psi(x,t+\Delta t) = \exp\left(\frac{i\Delta t}{\hbar}H\right)\Psi(x,t+\Delta t)\ . \tag{11.46}$$

A series expansion of the exponential results in the desired relation:

$$\Psi_k^n = \left(1 + \frac{i\Delta t}{\hbar}H\right)\Psi_k^{n+1}\ . \tag{11.47}$$

We emphasize that the unitarity of the time-evolution operator is of fundamental importance since it preserves the norm of the wave-function. However, in truncating the series representation of the unitary time evolution operator $U(\Delta t)$ we certainly violate the unitarity of $U(\Delta t)$. This problem can be remedied by imposing unitarity of the time evolution as an additional requirement. This requirement can be incorporated by normalizing the wave-function after each time step.

We demonstrate now that the CRANK-NICOLSON scheme [15] can be applied successfully to solve Eq. (11.40) numerically for a particular potential. The CRANK-NICOLSON scheme can be obtained by realizing that

$$\begin{aligned} U(\Delta t) &= \exp\left(-\frac{i\Delta t}{\hbar}H\right) \\ &= \exp\left(-\frac{i\Delta t}{2\hbar}H\right)\exp\left(-\frac{i\Delta t}{2\hbar}H\right) \\ &= \exp\left(\frac{i\Delta t}{2\hbar}H\right)^{-1}\exp\left(-\frac{i\Delta t}{2\hbar}H\right) \\ &= \left[U^{\dagger}\left(\frac{\Delta t}{2}\right)\right]^{-1}U\left(\frac{\Delta t}{2}\right)\ . \end{aligned} \tag{11.48}$$

Hence, we obtain from Eq. (11.45)

$$U^{\dagger}\left(\frac{\Delta t}{2}\right)\Psi_k^{n+1} = U\left(\frac{\Delta t}{2}\right)\Psi_k^n\ , \tag{11.49}$$

or by expanding U in a series and truncating after the second term

$$\left(1 + \frac{i\Delta t}{2\hbar}H\right)\Psi_k^{n+1} = \left(1 - \frac{i\Delta t}{2\hbar}H\right)\Psi_k^n\ . \tag{11.50}$$

Inserting the finite difference approximation of the Hamiltonian H and rearranging terms yields

$$\left[1+\frac{i\Delta t}{2\hbar}\left(\frac{\hbar^2}{m\Delta x^2}+V_k\right)\right]\Psi_k^{n+1}-\frac{i\Delta t\,\hbar}{4m\Delta x^2}\left(\Psi_{k-1}^{n+1}+\Psi_{k+1}^{n+1}\right)=\hat{\Omega}_k^n\,, \tag{11.51}$$

where we defined $\hat{\Omega}_k^n$ as

$$\hat{\Omega}_k^n=\left[1-\frac{i\Delta t}{2\hbar}\left(\frac{\hbar^2}{m\Delta x^2}+V_k\right)\right]\Psi_k^n+\frac{i\Delta t\,\hbar}{4m\Delta x^2}\left(\Psi_{k-1}^n+\Psi_{k+1}^n\right)\,. \tag{11.52}$$

Both sides of Eq. (11.51) are now multiplied by $i4m\Delta x^2/(\hbar\Delta t)$ and this gives

$$\Psi_{k-1}^{n+1}+2\left(\frac{i2m\Delta x^2}{\Delta t\,\hbar}-1-\frac{m\Delta x^2}{\hbar^2}V_k\right)\Psi_k^{n+1}+\Psi_{k+1}^{n+1}=\Omega_k^n\,, \tag{11.53}$$

where

$$\Omega_k^n=-\Psi_{k-1}^n+2\left(\frac{i2m\Delta x^2}{\Delta t\,\hbar}+1+\frac{m\Delta x^2}{\hbar^2}V_k\right)\Psi_k^n-\Psi_{k+1}^n\,. \tag{11.54}$$

We recognize that Eq. (11.53) establishes a system of linear equations and rewrite it in matrix form:

$$A\Psi^{n+1}=\Omega^n\,. \tag{11.55}$$

Here, we defined the vectors $\Psi^n=\left(\Psi_0^n,\Psi_1^n,\dots,\Psi_N^n\right)^T$, $\Omega^n=\left(\Omega_0^n,\Omega_1^n,\dots,\Omega_N^n\right)^T$ and the tridiagonal matrix

$$A=\begin{pmatrix} \ddots & \ddots & \ddots & & \\ & 1 & \Gamma_k & 1 & \\ & & \ddots & \ddots & \ddots \end{pmatrix}\,, \tag{11.56}$$

with Γ_k for $k=1,2,\dots,N$ given by

$$\Gamma_k=2\left(\frac{i2m\Delta x^2}{\Delta t\,\hbar}-1-\frac{m\Delta x^2}{\hbar^2}V_k\right)\,, \tag{11.57}$$

according to Eq. (11.53).

The system (11.56) is solved iteratively. However, in this case we employ a more elegant ansatz which is allowed for tridiagonal matrices. We set

$$\Psi_{k+1}^{n+1} = a_k \Psi_k^{n+1} + b_k^n \;, \tag{11.58}$$

and apply it to Eq. (11.53). After rearranging terms we arrive at:

$$2\left(1 + \frac{m\Delta x^2}{\hbar^2} V_k - \frac{i2m\Delta x^2}{\Delta t\,\hbar} - \frac{a_k}{2}\right) \Psi_k^{n+1} = \Psi_{k-1}^{n+1} + b_k^n - \Omega_k^n \;. \tag{11.59}$$

We define

$$\alpha_k = 2\left(1 + \frac{m\Delta x^2}{\hbar^2} V_k - \frac{i2m\Delta x^2}{\Delta t\,\hbar} - \frac{a_k}{2}\right) \;, \tag{11.60}$$

and obtain from Eq. (11.59)

$$\Psi_k^{n+1} = \frac{1}{\alpha_k} \Psi_{k-1}^{n+1} + \frac{b_k^n - \Omega_k^n}{\alpha_k} \;. \tag{11.61}$$

However, due to the ansatz (11.58) we also have

$$\Psi_k^{n+1} = a_{k-1} \Psi_{k-1}^{n+1} + b_{k-1}^n \;, \tag{11.62}$$

which results in the relations

$$a_{k-1} = \frac{1}{\alpha_k} \;, \tag{11.63}$$

and

$$b_{k-1}^n = \frac{b_k^n - \Omega_k^n}{\alpha_k} = \left(b_k^n - \Omega_k^n\right) a_{k-1} \;. \tag{11.64}$$

Equation (11.63) leads to the recursion relation

$$a_k = 2\left(1 + \frac{m\Delta x^2}{\hbar^2} V_k - \frac{i2m\Delta x^2}{\Delta t\,\hbar}\right) - \frac{1}{a_{k-1}} \;, \tag{11.65}$$

and we derive from Eq. (11.64):

$$b_k^n = \frac{b_{k-1}^n}{a_{k-1}} + \Omega_k^n \;. \tag{11.66}$$

The remaining question is how to choose a_0 and b_0^n. We impose the boundary conditions $\Psi_0^n = 0$ and $\Psi_N^n = 0$ and derive from Eq. (11.53):

$$\Omega_1^n = 2\left(\frac{i2m\Delta x^2}{\Delta t\hbar} - 1 - \frac{m\Delta x^2}{\hbar^2}V_1\right)\Psi_1^{n+1} + \Psi_2^{n+1} \ . \tag{11.67}$$

A comparison of this equation with the ansatz (11.58), i.e. $\Psi_2^{n+1} = a_1\Psi_1^{n+1} + b_1^n$, reveals that

$$a_1 = 2\left(1 + \frac{m\Delta x^2}{\hbar^2}V_1 - \frac{i2m\Delta x^2}{\Delta t\hbar}\right) \ , \tag{11.68}$$

and

$$b_1^n = \Omega_1^n \ . \tag{11.69}$$

These expressions are equivalent to $a_0 = \infty$ and it is, thus, impossible to calculate Ψ_1^{n+1} from Ψ_0^{n+1}. However, we can determine the function values Ψ_k^{n+1} via a backward recursion

$$\Psi_k^{n+1} = \frac{1}{a_k}\left(\Psi_{k+1}^{n+1} - b_k^n\right) \ , \tag{11.70}$$

which is initialized with the boundary condition $\Psi_N^{n+1} = 0$. We can now summarize the algorithm:

1. Choose the initial conditions Ψ_k^0, $k = 0, 1, \ldots, N$ which satisfy the boundary conditions $\Psi_0^0 = 0$ and $\Psi_N^0 = 0$.
2. Set

$$a_1 = 2\left(1 + \frac{m\Delta x^2}{\hbar^2}V_1 - \frac{i2m\Delta x^2}{\Delta t\hbar}\right) \ , \tag{11.71}$$

and calculate for $k = 2, \ldots, N-1$

$$a_k = 2\left(1 + \frac{m\Delta x^2}{\hbar^2}V_k - \frac{i2m\Delta x^2}{\Delta t\hbar}\right) - \frac{1}{a_{k-1}} \ . \tag{11.72}$$

3. Start the time loop: $n = 0, 1, \ldots, M$, with M the maximum number of time steps.
4. Calculate for $k = 1, 2, \ldots, N-1$

$$\Omega_k^n = -\Psi_{k-1}^n + 2\left(\frac{i2m\Delta x^2}{\Delta t\hbar} + 1 + \frac{m\Delta x^2}{\hbar^2}V_k\right)\Psi_k^n - \Psi_{k+1}^n \ . \tag{11.73}$$

5. Set

$$b_1^n = \Omega_1^n \, , \tag{11.74}$$

and calculate for $k = 2, \ldots, N-1$

$$b_k^n = \frac{b_{k-1}^n}{a_{k-1}} + \Omega_k^n \, . \tag{11.75}$$

6. Calculate for $k = N-1, N-2, \ldots, 1$

$$\Psi_k^{n+1} = \frac{1}{a_k} \left(\Psi_{k+1}^{n+1} - b_k^n \right) \, , \tag{11.76}$$

where the boundary conditions $\Psi_0^n = \Psi_N^n = 0$ are to be considered.

7. Set $n = n + 1$ and go to step 4.

The application of this algorithm is now elucidated with the help of a specific example, the quantum mechanical tunneling effect. The initial condition is described by a GAUSS wave packet

$$\Psi(x, 0) = \exp(iqx) \exp\left[-\frac{(x - x_0)^2}{2\sigma^2} \right] \, , \tag{11.77}$$

centered at $x = x_0$ which propagates in positive x-direction with momentum q. This wave-function is not yet normalized. Furthermore, we regard the single potential barrier

$$V_1(x) = \begin{cases} V_0 & x \in [a, b] \, , \\ 0 & \text{elsewhere,} \end{cases} \tag{11.78}$$

or the double potential barrier

$$V_2(x) = \begin{cases} V_0 & x \in [a, b] \cup [c, d] \, , \\ 0 & \text{elsewhere.} \end{cases} \tag{11.79}$$

The scales and parameters are chosen in the following way: $L = 500$, $\Delta x = 1$, $\Delta t = 0.1, m = \hbar = 1, x_0 = 200, q = 2, \sigma = 20, V_0 = 0.7, a = 250, b = 260, c = 300$, and $d = 310$. Figure 11.8 presents the time evolution of the square modulus of the resulting wave-function $|\Psi(x, n\Delta t)|^2$ vs x (solid line, left hand scale) at different time steps $n = 500$, 1000, and 1500. The time step $n = 0$ corresponds to the initial

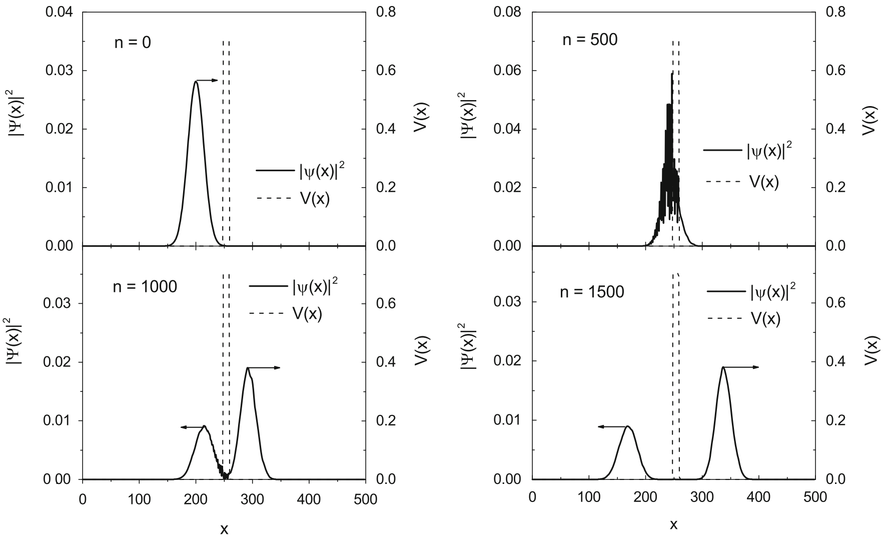

Fig. 11.8 Time evolution of the square modulus of the wave-function $|\psi(x)|^2$ vs x (*solid line, left hand scale*). The potential $V(x) = V_1(x)$ is also plotted vs x (*dashed line, right hand scale*). We present the results for $n = 500$, 1000, and 1500 time steps. The graph labeled by $n = 0$ represents the initial configuration

condition. The potential $V_1(x)$ vs x is also plotted (dashed line, right hand scale). Figure 11.9 corresponds to Fig. 11.8 but now the potential is described by $V_2(x)$ and additional time steps for $n = 2000$ and 2500 have been added.

In both figures a typical quantum mechanical effect which is referred to as *tunneling* can be observed. In particular, there exists a finite probability that the potential barrier can be crossed, although, from a classical point of view, the particle's energy is not sufficient to overcome the barrier. A detailed discussion of this effect and its technological importance can be found in any standard textbook on quantum mechanics [19–21].

In conclusion we remark that a very prominent method to solve numerically the time-dependent SCHRÖDINGER equation is based on the FOURIER transformation. The numerical implementation of the FOURIER transformation as well as its application to the SCHRÖDINGER equation is briefly discussed in Appendix D.

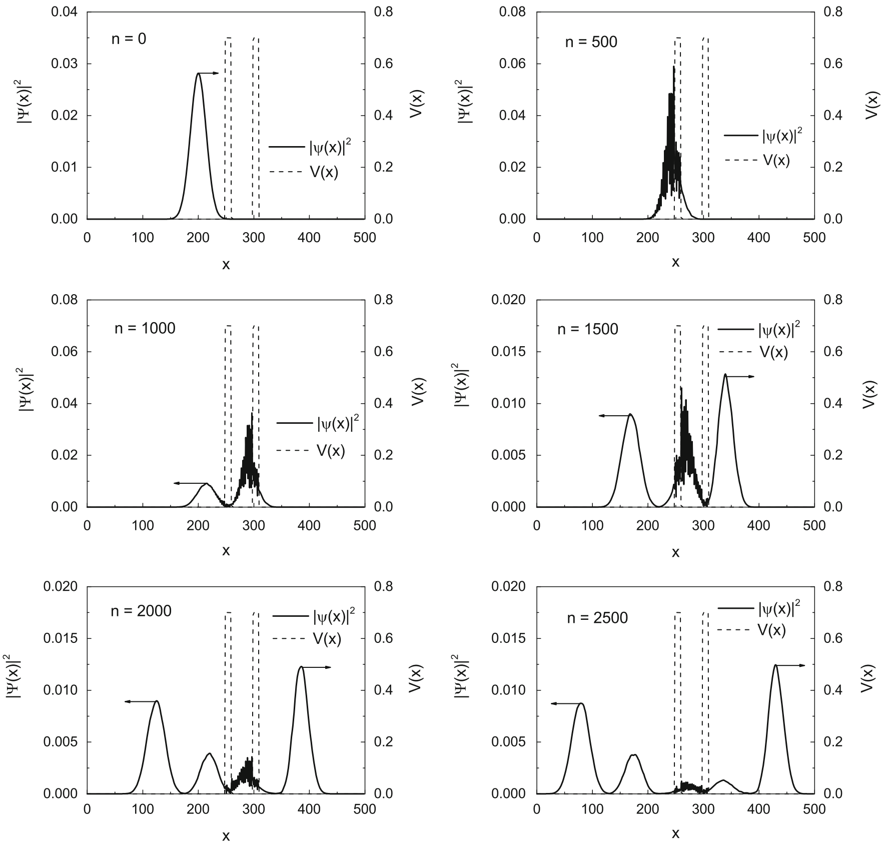

Fig. 11.9 Time evolution of the square modulus of the wave-function $|\psi(x)|^2$ vs x (*solid line, left hand scale*). The potential $V(x) = V_2(x)$ is also plotted vs x (*dashed line, right hand scale*). We present the results for $n = 500$, 1000, 1500, 2000, and 2500 time steps. The graph labeled by $n = 0$ represents the initial configuration

Summary

This chapter was about linear PDEs and how to find solutions numerically. The dominating theme was the application of the various finite difference methods. The two-dimensional POISSON equation served as an example for an elliptic PDE. The algorithm to solve this equation developed here was based on the central difference derivative. Parabolic PDEs were represented by the time-dependent one-dimensional heat equation. The numerical solution proved to be possible by either using an explicit or an implicit EULER scheme. For the explicit EULER scheme the appropriate choice of time and space discretization proved to be essential for the stability of the algorithm. The one-dimensional wave equation was introduced as an example of a hyperbolic PDE. The solution was found by employing an explicit

EULER approximation. Again time and space discretization had to follow a specific stability criterion, the COURANT-FRIEDRICHS-LEWY condition. Finally, the one-dimensional time-dependent SCHRÖDINGER equation was studied. It does not fit into any of the above categories. The algorithm to find a numerical solution was developed here on the basis of a CRANK-NICOLSON scheme and it was tested with the quantum mechanical tunneling effect.

Problems

1. Write a program which solves the two-dimensional POISSON equation for an arbitrary charge density distribution $\rho(x, y)$. Use the numerical method discussed in Sect. 11.2.

   a. Impose DIRICHLET boundary conditions $\varphi(x, 0) = \varphi(x, L_y) = \varphi(0, y) = \varphi(L_x, y) = 0$ as described in Sect. 11.2. Test the program by first reproducing Fig. 11.2.
   b. Solve the POISSON equation for different charge densities of your choice.
   c. Calculate the electric field $E(x, y)$ with the help of Eq. (11.3).

2. Calculate the time evolution of the temperature distribution $T(x, t)$ along a cylindrical rod described in Sect. 9.3. The rod is kept at constant temperatures T_0 and T_N at its ends. The parameters used in Sect. 9.3 stay unchanged. Study also the case of a heat sink as suggested in the Problems section of Chap. 9.
3. Calculate the time evolution of the square modulus of the wave-function $|\psi(x)|^2$ vs x for a potential $V_1(x)$ according to Eq. (11.78) with $V_0 < 0$ (quantum well). In a second step, modify the potential according to

$$V(x) = \begin{cases} V_1 & x \in [a, b] \cup [c, d] \\ V_2 & x \in [b, c] \\ 0 & \text{elsewhere,} \end{cases}$$

   with $V_1 > 0$, $V_2 < 0$, and $|V_1| < |V_2|$.

References

1. Lapidus, L., Pinder, G.F.: Numerical Solution of Partial Differential Equations. Wiley, New York (1982)
2. Morton, K.W., Mayers, D.F.: Numerical Solution of Partial Differential Equations. Cambridge University Press, Cambridge (2005)
3. Li, T., Qin, T.: Physics and Partial Differential Equations, vol. 1. Cambridge University Press, Cambridge (2012)

4. Li, T., Qin, T.: Physics and Partial Differential Equations, vol. 2. Cambridge University Press, Cambridge (2014)
5. Lui, S.H.: Numerical Analysis of Partial Differential Equations. Wiley, New York (2012)
6. LeVeque, R.J.: Finite Volume Methods for Hyperbolic Problems. Cambridge Texts in Applied Mathematics. Cambridge University Press, Cambridge (2002)
7. Gockenbach, M.S.: Understanding and Implementing the Finite Element Method. Cambridge University Press, Cambridge (2006)
8. Selvadurai, A.: Partial Differential Equations in Mechanics, vol. 2. Springer, Berlin/Heidelberg (2000)
9. Sleeman, B.D.: Partial differential equations, poisson equation. In: Dubitzky, W., Wolkenhauer, O., Cho, K.H., Yokota, H. (eds.) Encyclopedia of Systems Biology, pp. 1635–1638. Springer, Berlin/Heidelberg (2013)
10. Jackson, J.D.: Classical Electrodynamics, 3rd edn. Wiley, New York (1998)
11. Greiner, W.: Classical Electrodynamics. Springer, Berlin/Heidelberg (1998)
12. Polyanin, A.D.: Handbook of Linear Partial Differential Equations for Engineers and Scientists. Chapman & Hall/CRC, Boca Raton (2002)
13. Cannon, J.R.: The One-Dimensional Heat Equation. Encyclopedia of Mathematics and Its Applications. Cambridge University Press, Cambridge (1985)
14. Carslaw, H.S., Jaeger, J.C.: Conduction of Heat in Solids, 2nd edn. Oxford University Press, Oxford (1986)
15. Crank, J., Nicolson, P.: A practical method for numerical evaluation of solutions of partial differential equations of the heat-conduction type. Proc. Camb. Philos. Soc. **43**, 50–67 (1947). doi:10.1017/S0305004100023197
16. Zwillinger, D.: Handbook of Differential Equations, 3nd edn. Academic, San Diego (1997)
17. Courant, R., Friedrichs, K., Lewy, H.: On the partial difference equations of mathematical physics. IBM J. Res. Dev. **11**, 215–234 (1967 [1928])
18. Bakhvalov, N.S.: Courant-friedrichs-lewy condition. In: Hazewinkel, M. (ed.) Encyclopaedia of Mathematics. Springer, Berlin/Heidelberg (1994)
19. Sakurai, J.J.: Modern Quantum Mechanics. Addison-Wesley, Menlo Park (1985)
20. Baym, G.: Lectures on Quantum Mechanics. Lecture Notes and Supplements in Physics. The Benjamin/Cummings Publ. Comp., Inc., London/Amsterdam (1969)
21. Cohen-Tannoudji, C., Diu, B., Laloë, F.: Quantum Mechanics, vol. I. Wiley, New York (1977)